Since January 2020 Elsevier has created a COVID-19 resource centre with free information in English and Mandarin on the novel coronavirus COVID-19. The COVID-19 resource centre is hosted on Elsevier Connect, the company's public news and information website.

Protein Expression and Purification 194 (2022) 106075

Contents lists available at ScienceDirect

Protein Expression and Purification

journal homepage: www.elsevier.com/locate/yprep

Addition of arginine hydrochloride and proline to the culture medium enhances recombinant protein expression in *Brevibacillus choshinensis*: The case of RBD of SARS-CoV-2 spike protein and its antibody

Ryo Matsunaga [a], Kouhei Tsumoto [a,b,c,*]

[a] Department of Bioengineering, School of Engineering, The University of Tokyo, Tokyo, 113-8656, Japan
[b] Department of Chemistry and Biotechnology, School of Engineering, The University of Tokyo, Tokyo, 113-8656, Japan
[c] The Institute of Medical Science, The University of Tokyo, Tokyo, 108-8639, Japan

ARTICLE INFO

Keywords:
Brevibacillus
CoV-2
RBD
Antibody
High-throughput expression and purification

ABSTRACT

Brevibacillus choshinensis is a gram-positive bacterium that is known to efficiently secrete recombinant proteins. However, the expression of these proteins is often difficult depending upon the expressed protein. In this study, we demonstrated that the addition of arginine hydrochloride and proline to the culture medium dramatically increased protein expression. By culturing bacterial cells in 96-well plates, we were able to rapidly examine the expression conditions and easily scale up to 96 mL of culture for production. Although functional expression of the receptor binding domain (RBD) of the SARS-CoV-2 spike protein without any solubility-enhancing tag in bacterial strains (including *Escherichia coli*) has not been reported to date, we succeeded in efficiently producing RBD which showed a similar CD spectrum to that of RBD produced by eukaryotic cell expression systems. Furthermore, RBD from the omicron variant (B.1.1.529) was also produced. Physicochemical analyses indicated that omicron RBD exhibited markedly increased instability compared to the wild-type. We also revealed that the Fab format of the anti-SARS-CoV-2 antibody C121 can be produced in large quantities using the same expression system. The obtained C121 Fab bound to wild-type RBD but not to omicron RBD. These results strongly suggest that the *Brevibacillus* expression system is useful for facilitating the efficient expression of proteins that are difficult to fold and will thus contribute to the rapid physicochemical evaluation of functional proteins.

1. Introduction

Bacterial expression systems have been widely used in the research and pharmaceutical fields based on their ability to produce recombinant proteins easily and at a low cost. *Escherichia coli* has been used for a long period of time, and various expression vectors and methods to allow for functional expression have been developed [1,2]. In many cases, proteins containing disulfide bonds are expressed in the periplasm by fusion with a signal peptide [3] owing to the reductive environment of the cytoplasm. However, the efficiency of secretory expression in *E. coli* is low. Furthermore, endotoxin contamination is often a problem in certain applications [4].

Brevibacillus is a soil-derived gram-positive bacterium that is known for its superior ability to secrete proteins without endotoxin [5]. The expression system utilizing *Brevibacillus choshinensis* (*B. choshinesis*) is commercially available [6], and the expression of various types of proteins such as enzymes, cytokines, and antibodies has been previously reported [7–18]. However, in our experience, the expression levels of some proteins are often insufficient or decrease when scaled up from the test tube to the flask. It has been reported that optimization of the medium composition by including peptone and carbon sources [11] or the addition of magnesium chloride [14], proline [11], or arginine hydrochloride (ArgHCl) [18] to the medium improves protein expression. However, these methods may be limited by their application to specific proteins and are not generalizable. Additionally, although it has been determined that jar fermenters can be used for mass production of proteins, these systems are not suitable for the simultaneous production of various proteins for biochemical research applications.

In this study, we developed an efficient method to examine expression conditions by adding folding auxiliary molecules to the culture medium. For this purpose, we attempted to culture cells in 96-well plates to allow for number of different medium conditions to be examined

* Corresponding author. Department of Bioengineering, School of Engineering, The University of Tokyo, Tokyo, 113-8656, Japan.
E-mail address: tsumoto@bioeng.t.u-tokyo.ac.jp (K. Tsumoto).

https://doi.org/10.1016/j.pep.2022.106075
Received 11 February 2022; Received in revised form 22 February 2022; Accepted 23 February 2022
Available online 26 February 2022

simultaneously. For production, we incorporated 96 mL of culture into 96-well plates under the same optimized conditions and successfully expressed and purified the proteins from the culture supernatant.

We focused on the receptor-binding domain (RBD) of the SARS-CoV-2 spike protein as the target of this research. Since the beginning of the 2019 SARS-CoV-2 pandemic, RBD that is the key domain for human cell infection [19,20] has attracted much attention as a target molecule for treatment utilizing neutralizing antibodies [21,22] and vaccines [23]. In this context, recombinant expression of RBD in *E. coli* has been attempted; however, expression without the presence of any solubility-enhancing tag within the soluble fraction and with correct folding has not yet been achieved [24–32]. RBD possesses four disulfide bonds [33] that make it difficult for this domain to fold correctly. Although many attempts have been made to refold RBDs from inclusion bodies, the procedure is complicated, and it has been suggested that the physicochemical properties may differ from those of proteins produced by baculovirus or by mammalian cell expression systems [31]. Although the RBD-MBP fusion protein was reported to be expressed in the soluble fraction of the cytoplasm [32], there was no structural or physicochemical information for the recombinant fusion protein except for information regarding ACE2 binding ability, and it may be possible that untagged RBD is insoluble when MBP is cleaved due to the strong solubilizing effect of MBP [34].

As SARS-CoV-2 continues to mutate, a bacterial expression system capable of high-throughput expression of RBD possessing correct folding will be beneficial for physicochemical analysis of the mutants. For this purpose, we also attempted to create recombinant RBD from the omicron variant (B.1.1.529) that possesses 15 mutations in RBD [35] and to compare the physicochemical properties of this mutant to those of the wild type.

Furthermore, we also examined the production of the Fab format of the anti-RBD antibody C121 [36] in *B. choshinesis* to confirm the generality of our strategy. Although Fab antibody production in *B. choshinesis* has been reported using a duet vector harboring tandem VL-CL and VH-CH1 genes, there are likely more optimal medium conditions for production. Additionally, omicron RBD possesses an E484A mutation that was reported to function as an escape mutation from C121 [37,38]. Therefore, we hypothesized that we could obtain suggestions for the function and folding of recombinant proteins by analyzing the interactions between these proteins.

2. Materials and methods

2.1. Optimization of recombinant protein expression

The nucleotide sequences for the SARS-CoV-2 spike RBD (wild-type and omicron: aa 319–537) and Fab format of anti-RBD antibody C121 were codon-optimized and synthesized by Integrated DNA Technologies, Inc. They were then inserted into the pBIC4 vector (TaKaRa Bio) or the pNI vector (TaKaRa Bio). In the C121 Fab expression vector, the signal peptide sequence of VL-CL was from pBIC3 (TaKaRa Bio) and that of VH-VH1 was from pBIC4. The plasmid maps are presented in Fig. 1A and 3A. The plasmids were transformed into *Brevibacillus* competent cells (TaKaRa Bio) and cultured at 37 °C in TM medium to create a glycerol stock of the cells. Glycerol stock (10 μL) was added to each well of a 96-well deep-well plate containing 1 mL of medium. TM and 2SY media containing neomycin were used as basic media. The 2SY medium contained 20 g/L of glucose, 40 g/L of Phytone Peptone (Thermo Fisher Scientific), 5 g/L of Bacto Yeast Extract (Thermo Fisher Scientific), and 0.11 g/L of $CaCl_2$. TM medium contained 10 g/L of glucose, 10 g/L of Phytone Peptone (Thermo Fisher Scientific), 5 g/L of 35% Ehrlich Bonito Extract (Kyokuto Pharmaceutical), 2 g/L of Yeast extract SH (Fujifilm Wako Pure Chemicals), 10 mg/L of $FeSO_4 \cdot 7H_2O$, 8.9 mg/L of $MnCl_2 \cdot 4H_2O$, and 1 mg/L of $ZnSO_4 \cdot 7H_2O$. Proline (10 g/L) and/or ArgHCl (200 mM) was added to the basic medium. The plate was covered by a gas permeable seal and incubated at 1000 rpm at 30 °C for 60 h in a plate incubator (MBR-032P, TAITEC). Supernatants from each well were collected after performing a round of centrifugation at 20,000 *g* for 5 min, and they were subsequently used for SDS-PAGE analysis.

2.2. Expression and purification of RBD

The 2SY medium was supplemented with 10 g/L proline and 200 mM ArgHCl, and 1 mL of the glycerol stock of the transformed *B. choshinesis* was added to each well of a 96-well deep-well plate. The plate was covered by a gas permeable seal and incubated at 1000 rpm at 30 °C for 60 h in a plate incubator (MBR-032P, TAITEC). Supernatants were collected after performing a round of centrifugation at 40,000 *g* for 20 min and then sanitized by filtering. The supernatants were mixed at a 1:1 ratio with 200 mM Tris-HCl and 500 mM NaCl (pH 7.4) and then loaded onto a Ni Sepharose Excel (Cytiva) column. The column was washed with wash buffer composed of 20 mM Tris-HCl, 500 mM NaCl, and 20 mM imidazole (pH 7.4). His_6-tagged RBD was eluted using an elution buffer composed of 20 mM Tris-HCl, 500 mM NaCl, and 200 mM imidazole (pH 7.4). The His_6-tag of RBD was cleaved using TEV protease. RBD was further purified using SEC with a HiLoad 16/60 Superdex 200 pg column (GE Healthcare) or HiLoad 16/60 Superdex 75 pg column (GE Healthcare) that was equilibrated with phosphate-buffered saline (PBS). The monomer fraction was then collected. The elution profile of the proteins was monitored at 280 nm.

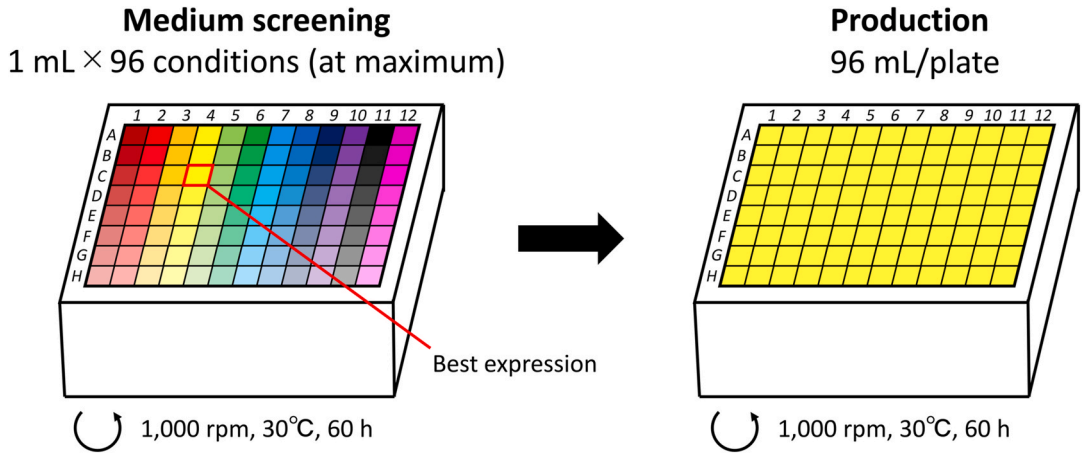

Fig. 1. High-throughput expression optimization and production system proposed in this study.

2.3. Expression and purification of C121 Fab

TM medium that was supplemented with 10 g/L of proline, 200 mM ArgHCl, and 1 mL of glycerol stock of the transformed *B. choshinesis* was added to each well of a 96-well deep-well plate. The plate covered by a gas permeable seal and incubated at 1000 rpm at 30 °C for 60 h in a plate incubator (MBR-032P, TAITEC). Supernatants were collected after performing a round of centrifugation at 40,000 *g* for 20 min and then sanitized by filtering. The supernatants were mixed at a 1:1 ratio with 200 mM Tris-HCl and 500 mM NaCl (pH 7.4) and then loaded onto a Ni Sepharose Excel (Cytiva) column. The column was washed with wash buffer composed of 20 mM Tris-HCl, 500 mM NaCl, and 20 mM imidazole (pH 7.4). His_6-tagged C121 Fab was eluted using an elution buffer composed of 20 mM Tris-HCl, 500 mM NaCl, and 200 mM imidazole (pH 7.4). His_6-tagged C121 Fab was further purified using SEC with a HiLoad 16/60 Superdex 200 pg column (GE Healthcare) that was equilibrated with PBS. The monomer fraction was then collected. The elution profile of the proteins was monitored at 280 nm.

2.4. Circular dichroism analysis

CD spectroscopy experiments were performed using a J-820 CD spectrometer (JASCO). Proteins were used at a concentration of 0.2 mg/ml. A quartz cuvette possessing a path length of 1 mm was used. Spectra were collected at 25 °C (resolution; 0.1 nm, average time: 4 s, scan speed: 50 nm/min) and obtained by calculating the average of four scans acquired from 260 to 200 nm. For thermal melting of RBD, the temperature was increased from 20 to 80 °C at a rate of 1 K/min, and signals at 210 nm were collected at 0.1 K intervals. The obtained thermal denaturation curves were fitted to a two-state transition model using JASCO software to obtain the thermodynamic parameters T_m and ΔH_{VH}.

2.5. Differential scanning calorimetry analysis

The heat capacity curves were measured using a MicroCal PEAQ-DSC instrument (Malvern). The samples were prepared in PBS at a monomer concentration of 1.0 mg/mL (the first sample) or 0.85 mg/mL (the second sample) for the wild-type RBD and at 0.76 mg/mL (the first sample) or 0.32 mg/mL (the second sample) for the omicron RBD. The scan rate was set to 1 K/min. Data were analyzed using MicroCal PEAQ-DSC software (Malvern). To obtain the thermodynamic parameters T_m and ΔH_{cal}, we subtracted the contribution of the buffer, normalized it according to the protein concentration, and fitted the data to a non-two-state model.

2.6. Biolayer interferometry analysis

The association and dissociation kinetics were analyzed using the Octet RED 384 System (Sartorius). His_6-tagged C121 Fab was diluted to 10 μg/mL with PBS containing 0.005 (v/v) % Tween 20 and then immobilized on anti-Penta-HIS biosensors (Sartorius). Measurements were performed in PBS containing 0.005 (v/v) % Tween 20 at 25 °C at a rotation rate of 1000 rpm. RBD was introduced as an analyte using a 2-fold dilution series of six steps over a concentration range of 1–32 nM. Data were analyzed using Octet Data Analysis software (Sartorius). Values in the absence of antibodies were subtracted from the data, and the curves were analyzed as 1:1 interaction kinetics.

3. Results

3.1. Construction of a high-throughput expression optimization system

We determined that culture using deep-well plates was effective for the growth and recombinant expression of *B. choshinesis*. Compared to culturing incorporating the use of test tubes, this method saves space and allows for simultaneous culturing under multiple conditions. Additionally, it is sufficient in most cases in the biochemical research field to obtain approximately 1 mg of the recombinant protein, an amount that can be expressed in a 96 mL culture of *B. choshinesis* in many cases. Therefore, we constructed a high-throughput expression optimization and production system as illustrated in Fig. 1. This system consists of two steps that include medium screening and production. In the first step, up to 96 conditions can be simultaneously tested using a single plate. The amount of expression was determined by SDS-PAGE or other techniques. After determining the medium composition in which recombinant expression is maximum, cultivation can be performed at a 96 mL scale for the production of the recombinant protein using a plate containing identical medium in all wells.

3.2. Optimization of RBD expression and purification

As the first model of this system, we chose the RBD of the spike protein of CoV-2. We constructed an expression vector for the wild-type RBD as presented in Fig. 2A. The TEV protease cleavage site was inserted between the His_6-tag and RBD to obtain an untagged RBD. To express recombinant RBD, we tested basic media for *B. choshinesis*, TM, and 2SY. However, the expression levels were too low (Fig. 2B, lanes 1 and 5), although slight expression was confirmed by western blotting analysis (data not shown). To optimize the culture conditions, we tested the effects of proline and ArgHCl. We selected these molecules due to their well characterized function as folding auxiliary molecules and based on reports indicating that they are effective for recombinant expression of certain types of proteins in *B. choshinesis* [11,18]. Eight medium conditions were screened using eight wells of a 96-well plate (Fig. 2B). RBD was expressed at high levels only in 2SY medium containing both proline and ArgHCl (Fig. 2B, lane 4).

Next, RBD was expressed under optimized conditions in a 96 mL of medium using a deep well plate. RBD was purified from the culture supernatant by immobilized metal affinity chromatography that was followed by cleavage of the His_6-tag by TEV protease. Finally, the RBD was subjected to size-exclusion chromatography (SEC). The chromatogram revealed that RBD existed exclusively as a monomer (Fig. 2C and D lane1). The final yield of the monomer fraction was approximately 1 mg per 96 mL of culture.

In addition to wild-type RBD, omicron RBD was expressed and purified using the same protocol. Although the expression level was lower than that for the wild type, we obtained a highly pure omicron RBD solution (Fig. 2D lane2).

3.3. Physicochemical properties of the recombinant RBD

CD spectral analyses were conducted to assess the folding of the recombinant RBD (Fig. 3A). The wild-type and omicron RBD exhibited the same characteristic spectra with a weak positive peak at approximately 232 nm and a strong negative peak at approximately 208 nm. This characteristic shape is the same as the reported CD spectra of recombinant RBDs produced by other expression systems. Thermal denaturation of the secondary structure was measured using a CD signal at 210 nm (Fig. 3B). Denaturation of the wild-type began at approximately 45 °C, and the T_m was calculated by fitting to a two-state transition model was 54.1 °C. In contrast, denaturation of the omicron RBD began at approximately 40 °C, and the T_m was 42.5 °C. This indicated that the omicron RBD was more unstable compared to the wild-type (Table 1).

Thermostability analysis was conducted using DSC. The heat capacity curves also clearly indicated that omicron RBD was remarkably unstable (Fig. 3C). The T_m of the wild-type was 49.7 °C, while that of the omicron RBD was 40.7 °C. This indicated that the omicron is 9 °C less thermally unstable than is the wild-type (Table 1).

3.4. Optimization of C121 Fab expression and purification

As we determined that RBD could be produced properly in this

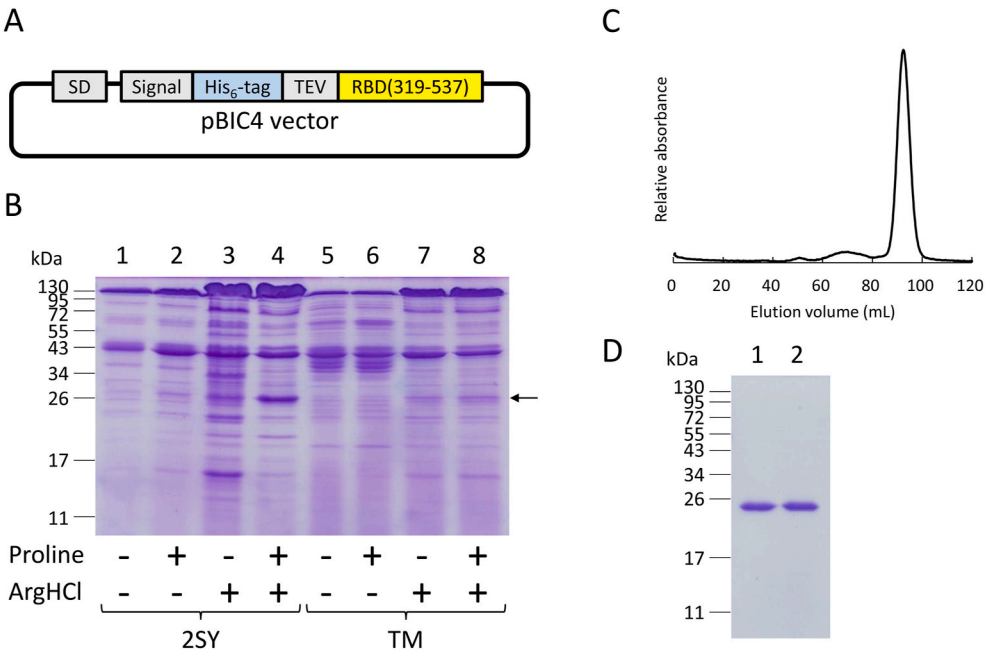

Fig. 2. Expression and purification of RBD. A, Vector map of the plasmid for RBD expression that was constructed in this study. B. Analysis of culture supernatants using 15% SDS-PAGE with Coomassie Brilliant Blue staining. Lane 1, 2SY medium; lane 2, 2SY medium supplemented with proline; lane 3, 2SY medium supplemented with ArgHCl; lane 4, 2SY medium supplemented with proline and ArgHCl; lane 5, TM medium; lane 6, TM medium supplemented with proline; lane 7, TM medium supplemented with ArgHCl; lane 8, TM medium supplemented with proline and ArgHCl. C, SEC elution profile of wild-type RBD. A HiLoad 16/60 Superdex 200 column was used. D. Analysis of purified recombinant RBD using 15% SDS-PAGE with Coomassie Brilliant Blue staining. Lane 1, wild-type RBD; lane 2, omicron RBD.

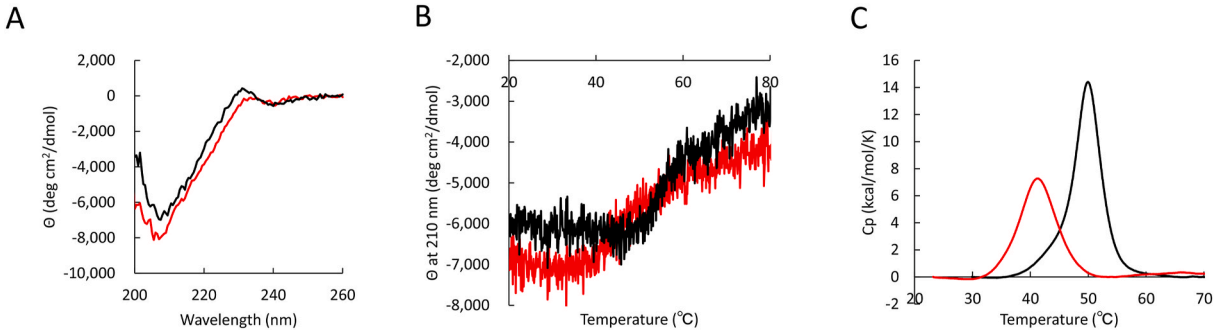

Fig. 3. Physicochemical properties of RBD. A, CD spectra. B, Thermal denaturation curves as measured by the CD signal at 210 nm. C, Heat capacity (C_p) curves as measured by DSC. Black, wild-type RBD; red, omicron RBD.

Table 1
Thermodynamic parameters of RBD.

	CD (n = 1)		DSC (n = 2)	
	T_m (°C)	ΔH_{VH} (kcal/mol)	T_m (°C)	ΔH_{cal} (kcal/mol)
WT	54.1	90	49.7	93
Omicron	42.5	48	40.7	59

expression system, we examined Fab antibodies as our next target. We constructed an expression vector for C121 Fab as presented in Fig. 4A. Fab is comprised of a heavy chain (VH–CH1) and a light chain (VL-CL), and the vector therefore contains these two genes. Similar to the experiments examining RBD, screening of medium conditions was conducted under eight conditions that included two basic medium compositions (TM and 2SY) with and without the addition of proline and ArgHCl. SDS-PAGE analysis of the culture supernatants revealed that TM medium containing ArgHCl (with or without proline) was the most optimal (Fig. 4B). *B. choshinesis* growth was remarkably suppressed, and extracellular expression of proteins, including C121 Fab, was quite low in the TM medium without proline and ArgHCl. In contrast, the expression of C121 Fab was evident in the 2SY medium; however, the addition of proline and/or ArgHCl was not as effective.

Based on the screening results, C121 Fab was expressed in TM medium supplemented with proline and ArgHCl in a deep well plate. C121 Fab was purified from the culture supernatant by immobilized metal affinity chromatography that was followed by SEC. The SEC chromatogram exhibited a single heterodimer peak that suggests the monodispersity of the solution (Fig. 2C and D lane1). The final yield of the peak fraction was approximately 10 mg per 96 mL of culture.

3.5. Physicochemical properties of the recombinant C121 Fab

The purified C121 Fab was subjected to CD analysis. The spectrum of C121 Fab exhibited a negative minimum at 218 nm that is typical of the immunoglobin fold. This result indicated that the C121 Fab underwent proper folding.

Finally, we conducted intermolecular interaction analysis between recombinant RBD and C121 Fab using biolayer interferometry (BLI). C121 Fab possessing a His_6-tag at the C-terminus of each chain was immobilized on the Anti-Penta-HIS Biosensors, and the interaction was measured using a serial dilution series of RBD solutions. The sensorgram revealed that C121 Fab bound to the wild-type RBD with a high affinity (K_D 3.25 nM) (Fig. 5B). Conversely, C121 Fab did not interact with the omicron RBD at concentrations below 32 nM (Fig. 5C), thus suggesting that the omicron strain would immunologically escape from this clone.

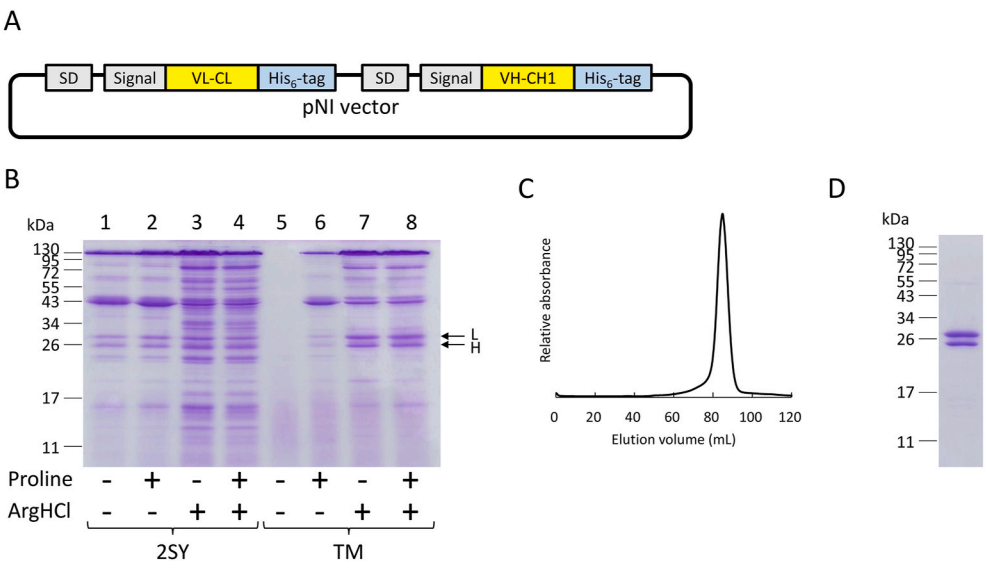

Fig. 4. Expression and purification of C121 Fab. A, Vector map of the plasmid used for the expression of C121 Fab that was constructed in this study. B. Analysis of culture supernatants using 15% SDS-PAGE with Coomassie Brilliant Blue staining. Lane 1, 2SY medium; lane 2, 2SY medium supplemented with proline; lane 3, 2SY medium supplemented with ArgHCl; lane 4, 2SY medium supplemented with proline and ArgHCl; lane 5, TM medium; lane 6, TM medium supplemented with proline; lane 7, TM medium supplemented with ArgHCl; lane 8, TM medium supplemented with proline and ArgHCl. C. SEC elution profile of C121 Fab. A HiLoad 16/60 Superdex 200 column was used. D. Analysis of purified recombinant C121 Fab using 15% SDS-PAGE with Coomassie Brilliant Blue staining.

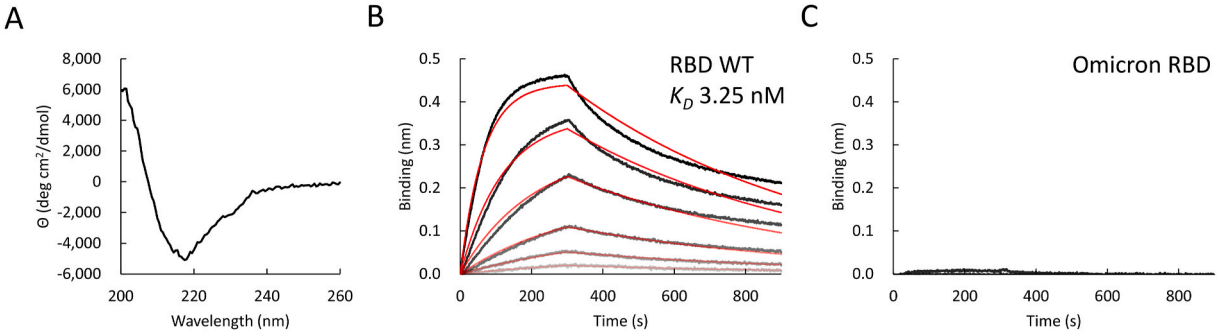

Fig. 5. Physicochemical properties of C121 Fab A, CD spectrum. B, C, BLI sensorgram. C121 Fab was immobilized on the sensors, and 1–32 nM of wild-type RBD (B) or omicron RBD (C) was used as the analyte. Black: raw data; red: fitting.

4. Discussion

In this study, we demonstrated that medium optimization is effective for the *B. choshinesis* expression system. We selected proline and ArgHCl as supplement candidates owing to their well characterized function as folding auxiliary molecules [39,40] and based on reports that they are effective for recombinant expression of certain types of proteins in *B. choshinesis* [11,18]. The results revealed that proline and ArgHCl synergistically enhanced RBD expression, thus indicating that they function through different mechanisms. We first hypothesized that they would assist in folding of the recombinant protein. However, the observation that they enhanced bacterial growth and the extracellular expression of intrinsic proteins indicated that they also exerted certain effects on cells as demonstrated in a previous study [11].

Even if these supplements are effective in some cases, it is almost impossible to predict the effect of other proteins. For example, their supplementation did not affect RBD expression in the TM medium, although they (particularly ArgHCl) were quite effective in regard to C121 Fab expression. Therefore, it is important to optimize the expression to simultaneously test the various conditions. In this context, our new strategy incorporating the use of 96-well plates would be helpful. Although we tested only proline and ArgHCl in this study, other additives (including metal ions and buffers) should be considered. We did not mention the signal sequence; however, it also significantly affected the expression level.

We believe that the culture system using 96-well plates is also convenient for producing a milligram scale of the recombinant protein. Although efficient high-throughput screening systems for *E.coli* [41,42] and *Pichia pastoris* [43] were already developed, this is the first report of using a 96-well plate as a culture container for production of recombinant protein for physicochemical analysis. If the culture flask is used, aeration and physical stress of the bacteria are very different from the 96-well plate system, and this may alter the expression level. We observed that the expression level was decreased when the bacteria were cultured in flasks, and we determined that the expression of the evident band at 45 kDa was also reduced (data not shown). This band was suggested to appear under stress conditions [44,45], and therefore, the 45 kDa protein may exert an effect on the expression and folding of recombinant proteins. When the culture for production is performed under the same conditions as those used for the optimization experiment, there is no such concern.

CoV-2 RBD has been reported to be recombinantly expressed in mammalian and insect cells and in *Pichia pastoris* [46,47]. However, to the best of our knowledge, no detailed characterization of recombinant RBDs expressed in bacteria is available. As the CD spectra and T_m of the wild-type RBD produced here resemble those of the reported RBD [46,47], it was suggested that our RBD underwent proper folding. The high-affinity interaction with C121 Fab, which has been shown to recognize the region overlapping epitope of ACE2 [36], also supports this argument. However, in order to reveal the accurate structure, it would be necessary to analyze 3D structure by X-ray crystallography or cryo-electric microscopy. In addition, it should be noted that the RBD expressed in *B. choshinesis* possesses no post-translational modifications, and this may affect some physicochemical properties. Therefore, careful

discussion is required when using this construct in biological experiments. We also demonstrated that the thermostability of the omicron RBD was 9 °C lower than was that of the wild-type. This observation is in agreement with a recently reported article that revealed omicron RBD expressed in mammarian cells was thermodynamically more unstable than wild-type [48]. Recently, crystal and cryoelectron microscopy structures of the omicron RBD-hACE2 complex were revealed [49]. According to the report, mutations alter the electrostatic surface of the ACE2-binding region, and this may lead to a decrease in thermostability.

5. Conclusion

We constructed a high-throughput system for optimizing the expression and production of recombinant proteins. Using this system, we could obtain CoV-2 RBD and anti-RBD Fab antibody. The recombinant proteins were suggested to fold correctly and to interact with each other. Furthermore, omicron RBD was also obtained and possessed different physicochemical properties compared to those of the wild-type.

Using this system, we expect to be able to express other proteins that are difficult to express in *E. coli*. Additionally, high-throughput physicochemical analysis is expected to enable rapid mutant analysis that will be useful for protein design.

Author statement

Ryo Matsunaga: Conceptualization, Methodology, Formal analysis, Investigation, Writing - Original Draft, Visualization, Funding acquisition. Kouhei Tsumoto: Conceptualization, Writing - Review & Editing, Supervision, Project administration, Funding acquisition.

Funding

This work was supported by JSPS KAKENHI Grant Number JP21K14737 and by JST CREST Grant Number JPMJCR20H8, Japan.

Declaration of competing interest

We have no conflicts of interest to be declared.

References

[1] J. Kaur, A. Kumar, J. Kaur, Strategies for optimization of heterologous protein expression in E. coli: roadblocks and reinforcements, Int. J. Biol. Macromol. 106 (2018) 803–822.
[2] G.L. Rosano, E.S. Morales, E.A. Ceccarelli, New tools for recombinant protein production in Escherichia coli: a 5-year update, Protein Sci. 28 (2019) 1412–1422.
[3] J.H. Choi, S.Y. Lee, Secretory and extracellular production of recombinant proteins using Escherichia coli, Appl. Microbiol. Biotechnol. 64 (2004) 625–635.
[4] S.K. Gupta, P. Shukla, Microbial platform technology for recombinant antibody fragment production: a review, Crit. Rev. Microbiol. 43 (2017) 31–42.
[5] H. Yamagata, K. Nakahama, Y. Suzuki, A. Kakinuma, N. Tsukagoshi, S. Udaka, Use of Bacillus-Brevis for efficient synthesis and secretion of human epidermal growth-factor, Proc. Natl. Acad. Sci. U.S.A. 86 (1989) 3589–3593.
[6] M. Mizukami, H. Hanagata, A. Miyauchi, Brevibacillus expression system: host-vector system for efficient production of secretory proteins, Curr. Pharmaceut. Biotechnol. 11 (2010) 251–258.
[7] K. Yashiro, J.W. Lowenthal, T.E. O'Neil, S. Ebisu, H. Takagi, R.J. Moore, High-level production of recombinant chicken interferon-gamma by Brevibacillus choshinensis, Protein Expr. Purif. 23 (2001) 113–120.
[8] Y. Yuki, C. Hara-Yakoyama, A.A. Guadiz, S. Udaka, H. Kiyono, S. Chatterjee, Production of a recombinant cholera toxin B subunit-insulin B chain peptide hybrid protein by Brevibacillus choshinensis expression system as a nasal vaccine against autoimmune diabetes, Biotechnol. Bioeng. 92 (2005) 803–809.
[9] Y.M. Cheng, M.T. Lu, C.M. Yeh, Functional expression of recombinant human trefoil factor 1 by Escherichia coli and Brevibacillus choshinensis, BMC Biotechnol. 15 (2015) 32.
[10] Y. Xu, W. Mao, W. Gao, Z. Chi, Z. Chi, G. Liu, Efficient production of a recombinant iota-carrageenase in Brevibacillus choshinensis using a new integrative vector for the preparation of iota-carrageenan oligosaccharides, Process Biochem. 76 (2019) 68–76.
[11] Z. Li, L. Su, X. Duan, D. Wu, J. Wu, Efficient expression of maltohexaose-forming alpha-amylase from Bacillus stearothermophilus in Brevibacillus choshinensis SP3 and its use in maltose production, BioMed Res. Int. 2017 (2017) 5479762.
[12] R. Tanaka, K. Kosugi, M. Mizukami, M. Ishibashi, H. Tokunaga, M. Tokunaga, Expression and purification of thioredoxin (TrxA) and thioredoxin reductase (TrxB) from Brevibacillus choshinensis, Protein Expr. Purif. 37 (2004) 385–391.
[13] C. Zou, X. Duan, J. Wu, Efficient extracellular expression of Bacillus deramificans pullulanase in Brevibacillus choshinensis, J. Ind. Microbiol. Biotechnol. 43 (2016) 495–504.
[14] C. Zou, X. Duan, J. Wu, Magnesium ions increase the activity of Bacillus deramificans pullulanase expressed by Brevibacillus choshinensis, Appl. Microbiol. Biotechnol. 100 (2016) 7115–7123.
[15] M. Mizukami, H. Onishi, H. Hanagata, A. Miyauchi, Y. Ito, H. Tokunaga, M. Ishibashi, T. Arakawa, M. Tokunaga, Efficient production of trastuzumab Fab antibody fragments in Brevibacillus choshinensis expression system, Protein Expr. Purif. 150 (2018) 109–118.
[16] H. Onishi, M. Mizukami, H. Hanagata, M. Tokunaga, T. Arakawa, A. Miyauchi, Efficient production of anti-fluorescein and anti-lysozyme as single-chain anti-body fragments (scFv) by Brevibacillus expression system, Protein Expr. Purif. 91 (2013) 184–191.
[17] M. Mizukami, H. Tokunaga, H. Onishi, Y. Ueno, H. Hanagata, N. Miyazaki, N. Kiyose, Y. Ito, M. Ishibashi, Y. Hagihara, T. Arakawa, A. Miyauchi, M. Tokunaga, Highly efficient production of VHH antibody fragments in Brevibacillus choshinensis expression system, Protein Expr. Purif. 105 (2015) 23–32.
[18] R. Asano, Y. Kuroki, S. Honma, M. Akabane, S. Watanabe, S. Mayuzumi, S. Hiyamuta, I. Kumagai, K. Sode, Comprehensive study of domain rearrangements of single-chain bispecific antibodies to determine the best combination of configurations and microbial host cells, mAbs 10 (2018) 854–863.
[19] N. Cuervo, N. Grandvaux, ACE2: evidence of role as entry receptor for SARS-CoV-2 and implications in comorbidities, Elife 9 (2020).
[20] C.B. Jackson, M. Farzan, B. Chen, H. Choe, Mechanisms of SARS-CoV-2 entry into cells, Nat. Rev. Mol. Cell Biol. 23 (2022) 3–20.
[21] S. Jiang, C. Hillyer, L. Du, Neutralizing antibodies against SARS-CoV-2 and other human coronaviruses, Trends Immunol. 41 (2020) 355–359.
[22] M. Yuan, H. Liu, N.C. Wu, I.A. Wilson, Recognition of the SARS-CoV-2 receptor binding domain by neutralizing antibodies, Biochem. Biophys. Res. Commun. 538 (2021) 192–203.
[23] Y. Valdes-Balbin, D. Santana-Mederos, F. Paquet, S. Fernandez, Y. Climent, F. Chiodo, L. Rodríguez, B. Sanchez Ramirez, K. Leon, T. Hernandez, L. Castellanos-Serra, R. Garrido, G.W. Chen, D. Garcia-Rivera, D.G. Rivera, V. Verez-Bencomo, Molecular aspects concerning the use of the SARS-CoV-2 receptor binding domain as a target for preventive vaccines, ACS Cent. Sci. 7 (2021) 757–767.
[24] X. Gao, S. Peng, S. Mei, K. Liang, M.S.I. Khan, E.G. Vong, J. Zhan, Expression and functional identification of recombinant SARS-CoV-2 receptor binding domain (RBD) from E. coli system, Prep. Biochem. Biotechnol. (2021) 1–7.
[25] M.L. Bellone, A. Puglisi, F. Dal Piaz, A. Hochkoeppler, Production in Escherichia coli of recombinant COVID-19 spike protein fragments fused to CRM197, Biochem. Biophys. Res. Commun. 558 (2021) 79–85.
[26] Q.D. Su, Y.N. Zou, Y. Yi, L.P. Shen, X.Z. Ye, Y. Zhang, H. Wang, H. Ke, J.D. Song, K. P. Hu, B.L. Cheng, F. Qiu, P.C. Yu, W.T. Zhou, R. Zhao, L. Cao, G.F. Dong, S.L. Bi, G. Z. Wu, G.F. Gao, J. Zheng, Recombinant SARS-CoV-2 RBD with a built in T helper epitope induces strong neutralization antibody response, Vaccine 39 (2021) 1241–1247.
[27] G.A. Fitzgerald, A. Komarov, A. Kaznadzey, I. Mazo, M.L. Kireeva, Expression of SARS-CoV-2 surface glycoprotein fragment 319-640 in E. coli, and its refolding and purification, Protein Expr. Purif. 183 (2021).
[28] Y. He, J. Qi, L. Xiao, L. Shen, W. Yu, T. Hu, Purification and characterization of the receptor-binding domain of SARS-CoV-2 spike protein from Escherichia coli, Eng. Life Sci. 21 (2021) 453–460.
[29] J.M. Errico, H. Zhao, R.E. Chen, Z. Liu, J.B. Case, M. Ma, A.J. Schmitz, M.J. Rau, J. A.J. Fitzpatrick, P.Y. Shi, M.S. Diamond, S.P.J. Whelan, A.H. Ellebedy, D. H. Fremont, Structural mechanism of SARS-CoV-2 neutralization by two murine antibodies targeting the RBD, Cell Rep. 37 (2021) 109881.
[30] A.R. Márquez-Ipiña, E. González-González, I.P. Rodríguez-Sánchez, I.M. Lara-Mayorga, L.A. Mejía-Manzano, M.G. Sánchez-Salazar, J.G. González-Valdez, R. Ortiz-López, A. Rojas-Martínez, G. Trujillo-de Santiago, M.M. Alvarez, Serological test to determine exposure to SARS-CoV-2: ELISA based on the receptor-binding domain of the spike protein (S-RBDN318-V510) expressed in Escherichia coli, Diagnostics 11 (2021).
[31] M. Maffei, L.C. Montemiglio, G. Vitagliano, L. Fedele, S. Sellathurai, F. Bucci, M. Compagnone, V. Chiarini, C. Exertier, A. Muzi, G. Roscilli, B. Vallone, E. Marra, The nuts and bolts of SARS-CoV-2 spike receptor-binding domain heterologous expression, Biomolecules 11 (2021).
[32] J. Prahlad, L.R. Struble, W.E. Lutz, S.A. Wallin, S. Khurana, A. Schnaubelt, M. J. Broadhurst, K.W. Bayles, G.E.O. Borgstahl, CyDisCo production of functional recombinant SARS-CoV-2 spike receptor binding domain, Protein Sci. 30 (2021) 1983–1990.
[33] J. Lan, J. Ge, J. Yu, S. Shan, H. Zhou, S. Fan, Q. Zhang, X. Shi, Q. Wang, L. Zhang, X. Wang, Structure of the SARS-CoV-2 spike receptor-binding domain bound to the ACE2 receptor, Nature 581 (2020) 215–220+.
[34] A. Malhotra, R. Burgess, M. Deutscher, Tagging for protein expression, Guide Prot. Purific. 463 (2009) 239–258.
[35] X. He, W. Hong, X. Pan, G. Lu, X. Wei, SARS-CoV-2 Omicron variant: characteristics and prevention, MedCommComm 2 (2021) 838–845.
[36] C.O. Barnes, C.A. Jette, M.E. Abernathy, K.A. Dam, S.R. Esswein, H.B. Gristick, A. G. Malyutin, N.G. Sharaf, K.E. Huey-Tubman, Y.E. Lee, D.F. Robbiani, M.

C. Nussenzweig, A.P. West, P.J. Bjorkman, SARS-CoV-2 neutralizing antibody structures inform therapeutic strategies, Nature 588 (2020) 682–687+.
[37] Y. Weisblum, F. Schmidt, F. Zhang, J. DaSilva, D. Poston, J.C. Lorenzi, F. Muecksch, M. Rutkowska, H.H. Hoffmann, E. Michailidis, C. Gaebler, M. Agudelo, A. Cho, Z. Wang, A. Gazumyan, M. Cipolla, L. Luchsinger, C.D. Hillyer, M. Caskey, D.F. Robbiani, C.M. Rice, M.C. Nussenzweig, T. Hatziioannou, P. D. Bieniasz, Escape from neutralizing antibodies by SARS-CoV-2 spike protein variants, Elife 9 (2020).
[38] R. De Gasparo, M. Pedotti, L. Simonelli, P. Nickl, F. Muecksch, I. Cassaniti, E. Percivalle, J.C.C. Lorenzi, F. Mazzola, D. Magrì, T. Michalcikova, J. Haviernik, V. Honig, B. Mrazkova, N. Polakova, A. Fortova, J. Tureckova, V. Iatsiuk, S. Di Girolamo, M. Palus, D. Zudova, P. Bednar, I. Bukova, F. Bianchini, D. Mehn, R. Nencka, P. Strakova, O. Pavlis, J. Rozman, S. Gioria, J.C. Sammartino, F. Giardina, S. Gaiarsa, Q. Pan-Hammarström, C.O. Barnes, P.J. Bjorkman, L. Calzolai, A. Piralla, F. Baldanti, M.C. Nussenzweig, P.D. Bieniasz, T. Hatziioannou, J. Prochazka, R. Sedlacek, D.F. Robbiani, D. Ruzek, L. Varani, Bispecific IgG neutralizes SARS-CoV-2 variants and prevents escape in mice, Nature 593 (2021) 424–428+.
[39] K. Tsumoto, M. Umetsu, I. Kumagai, D. Ejima, J.S. Philo, T. Arakawa, Role of arginine in protein refolding, solubilization, and purification, Biotechnol. Prog. 20 (2004) 1301–1308.
[40] D. Samuel, T.K. Kumar, G. Ganesh, G. Jayaraman, P.W. Yang, M.M. Chang, V. D. Trivedi, S.L. Wang, K.C. Hwang, D.K. Chang, C. Yu, Proline inhibits aggregation during protein refolding, Protein Sci. 9 (2000) 344–352.
[41] R.K.C. Knaust, P. Nordlund, Screening for soluble expression of recombinant proteins in a 96-well format, Anal. Biochem. 297 (1) (2001) 79–85.
[42] Y.P. Shih, W.M. Kung, J.C. Chen, C.H. Yeh, A.H.J. Wang, T.F. Wang, High-throughput screening of soluble recombinant proteins, Protein Sci. 11 (2002) 1714–1719.
[43] R. Weis, R. Luiten, W. Skranc, H. Schwab, M. Wubbolts, A. Glieder, Reliable high-throughput screening with Pichia pastoris by limiting yeast cell death phenomena, FEMS Yeast Res. 5 (2004) 179–189.
[44] M. Tokunaga, M. Mizukami, K. Yamasaki, H. Tokunaga, H. Onishi, H. Hanagata, M. Ishibashi, A. Miyauchi, K. Tsumoto, T. Arakawa, Secretory production of single-chain antibody (scFv) in Brevibacillus choshinensis using novel fusion partner, Appl. Microbiol. Biotechnol. 97 (2013) 8569–8580.
[45] D. Yao, K. Zhang, X. Zhu, L. Su, J. Wu, Enhanced extracellular alpha-amylase production in Brevibacillus choshinensis by optimizing extracellular degradation and folding environment, J. Ind. Microbiol. Biotechnol. 49 (2022).
[46] N.C. Dalvie, S.A. Rodriguez-Aponte, B.L. Hartwell, L.H. Tostanoski, A. M. Biedermann, L.E. Crowell, K. Kaur, O.S. Kumru, L. Carter, J. Yu, A. Chang, K. McMahan, T. Courant, C. Lebas, A.A. Lemnios, K.A. Rodrigues, M. Silva, R. S. Johnston, C.A. Naranjo, M.K. Tracey, J.R. Brady, C.A. Whittaker, D. Yun, N. Brunette, J.Y. Wang, C. Walkey, B. Fiala, S. Kar, M. Porto, M. Lok, H. Andersen, M.G. Lewis, K.R. Love, D.L. Camp, J.M. Silverman, H. Kleanthous, S.B. Joshi, D. B. Volkin, P.M. Dubois, N. Collin, N.P. King, D.H. Barouch, D.J. Irvine, J.C. Love, Engineered SARS-CoV-2 receptor binding domain improves manufacturability in yeast and immunogenicity in mice, Proc. Natl. Acad. Sci. U.S.A. 118 (2021).
[47] C. Arbeitman, G. Auge, M. Blaustein, L. Bredeston, E. Corapi, P. Craig, L. Cossio, L. Dain, C. D'Alessio, F. Elias, N. Fernandez, Y. Gandola, J. Gasulla, N. Gorojovsky, G. Gudesblat, M. Herrera, L. Ibanez, T. Idrovo, M. Rando, L. Kamenetzky, A. Nadra, D. Noseda, C. Pavan, M. Pavan, M. Pignataro, E. Roman, L. Ruberto, N. Rubinstein, J. Santos, F. Velazquez, A. Zelada, A.A. Consortium, A.A. Consortium, Structural and functional comparison of SARS-CoV-2-spike receptor binding domain produced in pichia pastoris and mammalian cells, Sci. Rep. 10 (2020) 21779.
[48] W. Yin, Y. Xu, P. Xu, X. Cao, C. Wu, C. Gu, X. He, X. Wang, S. Huang, Q. Yuan, K. Wu, W. Hu, Z. Huang, J. Liu, Z. Wang, F. Jia, K. Xia, P. Liu, B. Song, J. Zheng, H. Jiang, X. Cheng, Y. Jiang, S.J. Deng, H.E. Xu, Structures of the Omicron Spike trimer with ACE2 and an anti-Omicron antibody, Science (2022), eabn8863.
[49] P. Han, L. Li, S. Liu, Q. Wang, D. Zhang, Z. Xu, P. Han, X. Li, Q. Peng, C. Su, B. Huang, D. Li, R. Zhang, M. Tian, L. Fu, Y. Gao, X. Zhao, K. Liu, J. Qi, G.F. Gao, P. Wang, Receptor Binding and Complex Structures of Human ACE2 to Spike RBD from Omicron and Delta SARS-CoV-2, Cell, 2022.